SCIENTIFIC REPORTS

OPEN

Effective *W*-state fusion strategies for electronic and photonic qubits via the quantum-dot-microcavity coupled system

Received: 09 April 2015
Accepted: 09 July 2015
Published: 05 August 2015

Xue Han[1], Shi Hu[1], Qi Guo[2], Hong-Fu Wang[1], Ai-Dong Zhu[1] & Shou Zhang[1]

We propose effective fusion schemes for stationary electronic *W* state and flying photonic *W* state, respectively, by using the quantum-dot-microcavity coupled system. The present schemes can fuse a *n*-qubit *W* state and a *m*-qubit *W* state to a $(m+n-1)$-qubit *W* state, that is, these schemes can be used to not only create large *W* state with small ones, but also to prepare 3-qubit *W* states with Bell states. The schemes are based on the optical selection rules and the transmission and reflection rules of the cavity and can be achieved with high probability. We evaluate the effect of experimental imperfections and the feasibility of the schemes, which shows that the present schemes can be realized with high fidelity in both the weak coupling and the strong coupling regimes. These schemes may be meaningful for the large-scale solid-state-based quantum computation and the photon-qubit-based quantum communication.

Entanglement is a unique phenomenon in quantum mechanics, and it is an important quantum resource in the quantum information field. Especially, quantum entanglement plays a vital role in quantum communication and quantum information processing (QIP), such as quantum computation[1], quantum teleportation[2], quantum key distribution (QKD)[3], and so on. It is known to all that bipartite entanglement is different from multipartite entanglement. Among the multipartite entangled states, *W* state, GHZ state and cluster state form inequivalent classes and they can't be transformed into each other by local operations and classical communication. *W* state is a special kind of entangled state in the multipartite system. Compared with the GHZ state, *W* state is highly robust against the qubits loss. Hence, *W* state has recently attracted considerable attention in the field of quantum computing and information science[4–7]. For example, *W* state has been used for the optimal universal quantum cloning machine[8] and has also been proposed as a resource for QKD[9]. The more the number of particles forming an entangled state is, the more complex the entanglement structures are. Therefore the creation of multipartite entangled states has been paid much attention.

In the last decade, expansion and fusion operations have been proposed and demonstrated as efficient ways to prepare large scale multipartite entangled states. One can get a larger entangled state from two or more qubits entangled states by fusion operation on the condition that the access is granted only to one qubit of each of the states entering the fusion operation. Nowadays, much attention has been paid to the preparation of large scale multipartite entangled states by fusion operation. Currently, many expansion and fusion proposals of multipartite entangled states have been put forward, such as using cluster states with smaller-scale qubits to prepare larger cluster states[10], the creation of large-scale GHZ states[11] and *W* states[12–20]. Among those schemes, in 2011 Ozdemir *et al.* first used a simple optical fusion gate to get a *W* state W_{n+m-2} from W_n and W_m ($n,m \geq 3$ and W_x denotes a *x*-qubit *W* state)[16]. In the following years, they put forward several *W* states fusion schemes with the help of complex quantum gate sets. However,

[1]Department of Physics, College of Science, Yanbian University, Yanji, Jilin 133002, China. [2]Department of Physics, Harbin Institute of Technology, Harbin, Heilongjiang 150001, China. Correspondence and requests for materials should be addressed to S.Z. (email: szhang@ybu.edu.cn)

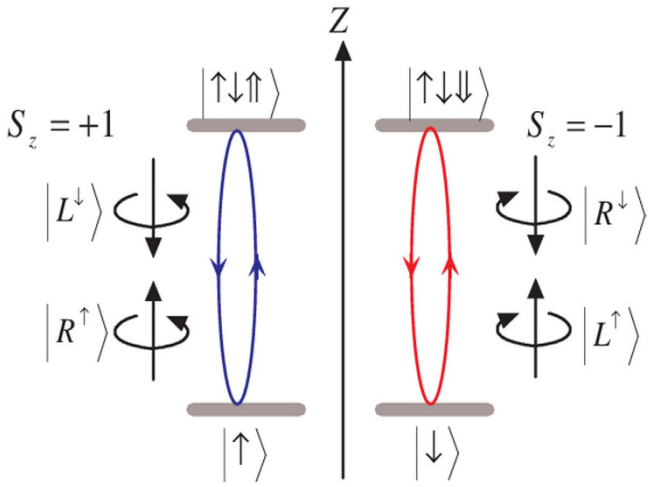

Figure 1. Relevant energy levels and optical selection rules for the optical transition of negatively charged exciton X^- in GaAs/InAs quantum dots embedded in an optical microcavity. The superscript arrows of the photon states indicates their propagation direction along or against the z axis.

multi-qubit controlled gates are great challenges for linear optical quantum computation[3]. Recently, we proposed a W-state fusion scheme without multi-qubit logical gates with the help of weak cross-Kerr nonlinearities[20].

Here, we respectively propose fusion schemes of electron-spin and polarized-photon W states with the help of quantum-dot(QD)-microcavity coupled system. Compared with the previous work[20], the present schemes not only propose the fusion scheme of polarized-photon W state, but also propose the fusion scheme of electron-spin W state, which can be used to solid-state-based quantum information processing. These schemes may be meaningful for the large-scale solid-state-based quantum computation and the photon-qubit-based quantum communication. In these schemes, only one particle of each multipartite entangled states is sent into the fusion device. After a series of operations, only one of the two particles is detected and the other is returned back to the state to prepare a $(m+n-1)$-qubit W state. Due to the developments in semiconductor nanoelectronics technology, QD-microcavity coupled system has been widely studied as a promising physical system for solid-state-based quantum information processing. So far, many efforts have been made such as fast initialization of the spin state of a single electron[21], nondestructive measurement[22], and fast optical control and coherent manipulation of a QD spin[23,24]. In recent years, a series of quantum information processing schemes based on QD-microcavity coupled system have been proposed[25–37]. All these works indicated that QD-microcavity coupled system is a good promising candidate and can be used for the storage and manipulation of quantum information. Therefore, it's meaningful to study the large-scale entanglement creation and fusion in the QD-microcavity system. Although the universal quantum gates can generate arbitrary entangled states, here we directly fuse the large-scale W states without any universal quantum gates which reduce the difficulty of experiment and can be achieved under the current experiment technology.

Results

Electronic *W*-state Fusion based on QD-microcavity coupled system. Here, we consider a singly charged GaAs/InAs QD, which has four relevant electronic levels, $|\uparrow\rangle$, $|\downarrow\rangle$, $|\uparrow\downarrow\Uparrow\rangle$, and $|\uparrow\downarrow\Downarrow\rangle$, as shown in Fig. 1, being embedded in a double-sided optical microcavity with both the top and bottom mirrors partially reflective. The negatively charged exciton (X^-), produced by the optical excitation of the system, contains two electrons bound in one hole. $|\Uparrow\rangle = \left|\frac{3}{2}, \frac{3}{2}\right\rangle$ and $|\Downarrow\rangle = \left|\frac{3}{2}, -\frac{3}{2}\right\rangle$ represent heavy hole states with spin 3/2 and $-3/2$ components. The total spin of the two electrons in an exciton is zero, which prevents the interaction between the electron-spin and the heavy hole spin. The quantization axis for angular momentum is the z axis because the quantum dot confinement potential is much tighter in the z(growth) direction than in the transversal direction due to the quantum dot geometry. According to this feature, it has two optical transitions between the electron state and the exciton state by involving the photon whose spin is $s_z = +1$ ($|R^{\uparrow}\rangle$ or $|L^{\downarrow}\rangle$) or $s_z = -1$ ($|R^{\downarrow}\rangle$ or $|L^{\uparrow}\rangle$). Based on the optical selection rules and the transmission and reflection rules of the cavity for an incident circular polarization photon, the interactions between photons and electrons in the QD-microcavity coupled system can be described as follows[26,27]:

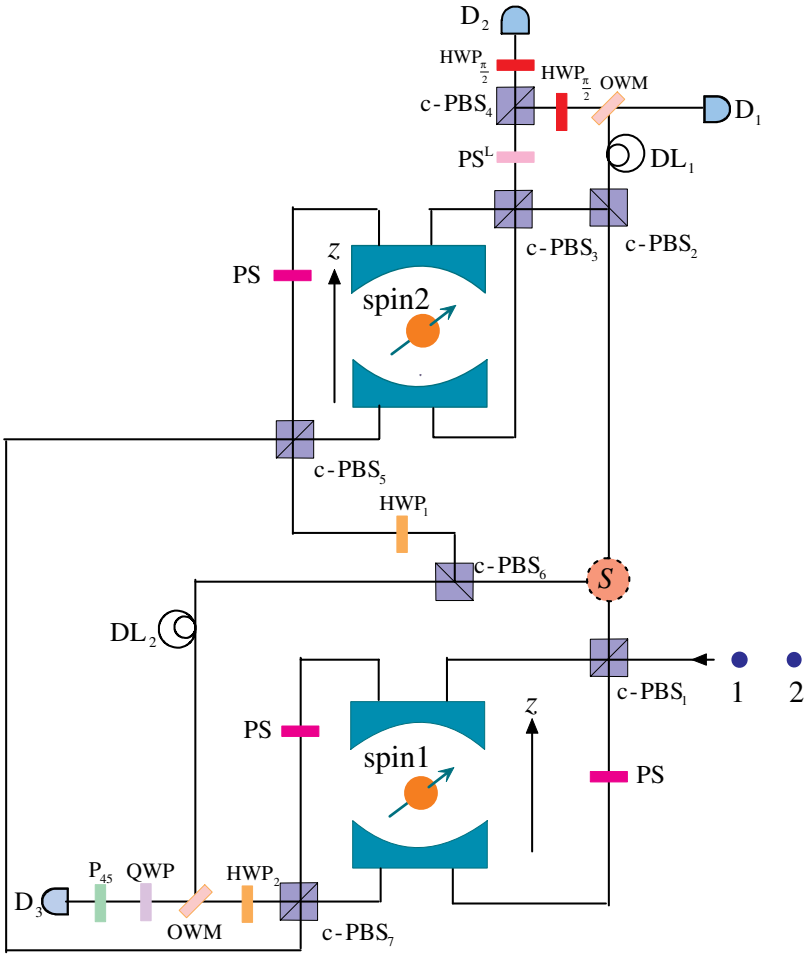

Figure 2. Schematic of electronic *W*-state. Spin 1 and spin 2 denote two QD spins coupled with two optical microcavities, respectively. c-PBS$_i$ (i = 1, 2, 3…): polarizing beam splitter in the circular basis. HWP$_i$ is half-wave plate, and HWP$_{\frac{\pi}{2}}$ implements the transformation $|R\rangle \leftrightarrow |L\rangle$. QWP: quarter-wave plate. S: optical switch. PS: π-phase shifter. The PS^L introduces a π phase for $|L\rangle$ and does not affect $|R\rangle$. OWM: one-way mirror transmits photons from one side, and reflects photons from the other side without remodulating. P$_{45}$ is a 45° polarizer projecting the polarization to $(|H\rangle + |V\rangle)/\sqrt{2}$. DL$_i$: the time-delay device for matching pathes length of the different components of the same photon. D$_i$: conventional photon detectors.

$$\begin{aligned}
&|R^{\uparrow}\uparrow\rangle \rightarrow |L^{\downarrow}\uparrow\rangle,\ |L^{\uparrow}\uparrow\rangle \rightarrow -|L^{\uparrow}\uparrow\rangle,\\
&|R^{\downarrow}\uparrow\rangle \rightarrow -|R^{\downarrow}\uparrow\rangle,\ |L^{\downarrow}\uparrow\rangle \rightarrow |R^{\uparrow}\uparrow\rangle,\\
&|R^{\uparrow}\downarrow\rangle \rightarrow -|R^{\uparrow}\downarrow\rangle,\ |L^{\uparrow}\downarrow\rangle \rightarrow |R^{\downarrow}\downarrow\rangle,\\
&|R^{\downarrow}\downarrow\rangle \rightarrow |L^{\uparrow}\downarrow\rangle,\ |L^{\downarrow}\downarrow\rangle \rightarrow -|L^{\downarrow}\downarrow\rangle. \qquad (1)
\end{aligned}$$

where $|R\rangle$ ($|L\rangle$) denotes the right(left)-circularly polarized photon state. The superscript up arrow (down arrow) denotes the propagating direction of polarized photon along (against) the z axis.

Now, we introduce how to implement a $(m+n-1)$ qubits electronic W-state fusion scheme from m qubits W state and n qubits W state based on QD-microcavity coupled system. The schematic is depicted in Fig. 2. We consider two spatially separated parties, Alice and Bob, who dominate two electronic entangled W states, $|W_n\rangle_A$ and $|W_m\rangle_B$, respectively, and decide to fuse their entangled states $|W_n\rangle_A$ and $|W_m\rangle_B$ to get a larger W state. The electronic W states of Alice and Bob can be denoted as[14]

$$\begin{aligned}
|W_n\rangle_A &= \frac{1}{\sqrt{n}}\left[\left|(n-1)_{\downarrow}\right\rangle_a |1_{\uparrow}\rangle_1 + \sqrt{n-1}\,|W_{n-1}\rangle_a \left|1_{\downarrow}\right\rangle_1\right]\\
&= |a\rangle|\uparrow\rangle_1 + |b\rangle|\downarrow\rangle_1, \qquad (2)
\end{aligned}$$

$$|W_m\rangle_B = \frac{1}{\sqrt{m}}\left[\left|(m-1)_\downarrow\right\rangle_b |1_\uparrow\rangle_2 + \sqrt{m-1}\,|W_{m-1}\rangle_b \left|1_\downarrow\right\rangle_2\right] = |c\rangle|\uparrow\rangle_2 + |d\rangle|\downarrow\rangle_2. \quad (3)$$

In this notation, a tripartite W state is written as $|W_3\rangle_A = \left(|\downarrow\downarrow\uparrow\rangle_A + |\downarrow\uparrow\downarrow\rangle_A + |\uparrow\downarrow\downarrow\rangle_A\right)/\sqrt{3} = \left(|2_\downarrow\rangle_a|1_\uparrow\rangle_1 + \sqrt{2}\,|W_2\rangle_a|1_\downarrow\rangle_1\right)/\sqrt{3}$ with $|W_2\rangle$ corresponding to the EPR pair $|W_2\rangle = (|\downarrow\uparrow\rangle + |\uparrow\downarrow\rangle)/\sqrt{2}$. For simplicity, here we have substituted $|a\rangle$ for $\left|(n-1)_\downarrow\right\rangle_a/\sqrt{n}$, $|b\rangle$ for $\sqrt{n-1}/\sqrt{n}\,|W_{n-1}\rangle_a$, $|c\rangle$ for $\left|(m-1)_\downarrow\right\rangle_b/\sqrt{m}$, and $|d\rangle$ for $\sqrt{(m-1)}/\sqrt{m}\,|W_{m-1}\rangle_b$. With the help of two ancillary photons in right-circular polarization state $|R\rangle$, we can fuse Alice's and Bob's electronic W states to a larger W state W_{m+n-1}. The initial state of the whole system is

$$|\Phi_0\rangle = |W_n\rangle_A \otimes |W_m\rangle_B \otimes |R_1\rangle \otimes |R_2\rangle = \left(|a\rangle|\uparrow\rangle_1 + |b\rangle|\downarrow\rangle_1\right) \otimes \left(|c\rangle|\uparrow\rangle_2 + |d\rangle|\downarrow\rangle_2\right)|R_1\rangle|R_2\rangle. \quad (4)$$

In the fusion process, only the electron spin 1 and 2 interaction with photons, the remaining electrons in modes a (b) are kept constant at Alice's (Bob's) side. Namely, only $|1_\uparrow\rangle_1|1_\uparrow\rangle_2$, $\left|1_\downarrow\right\rangle_1|1_\uparrow\rangle_2$, $|1_\uparrow\rangle_1\left|1_\downarrow\right\rangle_2$, and $\left|1_\downarrow\right\rangle_1\left|1_\downarrow\right\rangle_2$ interact with the photons, whose probabilities are $P_{\uparrow\uparrow} = 1/(nm)$, $P_{\downarrow\uparrow} = (n-1)/(nm)$, $P_{\uparrow\downarrow} = (m-1)/(nm)$, and $P_{\downarrow\downarrow} = (n-1)(m-1)/(nm)$, respectively.

Firstly, photon 1 passes through the c-PBS$_1$, which is polarizing beam splitter in the circular basis transmiting the right-circularly-polarized photon $|R\rangle$ and reflecting the left-circularly-polarized photon $|L\rangle$. That is, the components $|R_1\rangle$ and $|L_1\rangle$ enter the cavity 1 from the top and the bottom, respectively. PS is a phase shifter that contributes a π phase shift to the photon passing through it (i.e., $|L\rangle \to -|L\rangle$ and $|R\rangle \to -|R\rangle$). After the interaction with cavity 1, the components $|R_1\rangle$ and $|L_1\rangle$ mix at c-PBS$_1$ again. The above operations $\left(\text{c-PBS}_1 \to \left\{\begin{matrix}|\text{L}_1\rangle \to \text{PS} \to \text{spin 1}\\ |\text{R}_1\rangle \to \text{spin 1} \to \text{PS}\end{matrix}\right\} \to \text{c-PBS}_1\right)$ transform $|\Phi_0\rangle$ into

$$|\Phi_1\rangle = \Big[|a\rangle|R_1\rangle|\uparrow\rangle_1\left(|c\rangle|\uparrow\rangle_2 + |d\rangle|\downarrow\rangle_2\right) + |b\rangle|L_1\rangle|\downarrow\rangle_1\left(|c\rangle|\uparrow\rangle_2 + |d\rangle|\downarrow\rangle_2\right)\Big] \otimes |R_2\rangle. \quad (5)$$

Then, photon 1 gets to the optical switch (S) and goes toward the c-PBS$_2$. For the component $|L_1\rangle$, it passes through c-PBS$_3$ and enters cavity 2 to interact with spin 2. After that, it passes through the PS^L, c-PBS$_4$ and HWP$_{\frac{\pi}{2}}$ in turn. Here, the PS^L implements transformations $\{|L\rangle \to -|L\rangle, |R\rangle \to |R\rangle\}$ and HWP$_{\frac{\pi}{2}}$ is a half-wave plate oriented at 45° and realizes the transformation $|L\rangle \leftrightarrow |R\rangle$. That means the sate including component $|L_1\rangle$ after these operations (c-PBS$_2 \to$ c-PBS$_3 \to$ spin2 $\to$ PS$^L \to$ c-PBS$_4 \to$ HWP$_{\frac{\pi}{2}}$) becomes $\left(|b\rangle|c\rangle|R_1\rangle|\downarrow\rangle_1|\uparrow\rangle_2 + |b\rangle|d\rangle|L_1\rangle|\downarrow\rangle_1|\downarrow\rangle_2\right) \otimes |R_2\rangle$. While the component $|R_1\rangle$ transmits from c-PBS$_2$ and does not interact with the cavity. It passes c-PBS$_2 \to$ DL$_1 \to$ OWM in turn. DL is the time-delay device for matching path lengths of the two components. OWM is one-way mirror transmits photons from one side, and reflects photons from the other side without remodulating[38,39]. Hence, before the detectors click, the state will be

$$|\Phi_2\rangle = \left(|a\rangle|c\rangle|R_1\rangle|\uparrow\rangle_1|\uparrow\rangle_2 + |a\rangle|d\rangle|R_1\rangle|\uparrow\rangle_1|\downarrow\rangle_2 + |b\rangle|c\rangle|R_1\rangle|\downarrow\rangle_1|\uparrow\rangle_2 + |b\rangle|d\rangle|L_1\rangle|\downarrow\rangle_1|\downarrow\rangle_2\right) \otimes |R_2\rangle. \quad (6)$$

It is obvious that when the detector D$_2$ detects photon, the state is

$$|\phi_1\rangle = |b\rangle|d\rangle|\downarrow\rangle_1|\downarrow\rangle_2 \otimes |R_2\rangle. \quad (7)$$

In this case, we will obtain two separate W states with a smaller number of qubits, $|W_{n-1}\rangle$ and $|W_{m-1}\rangle$, which can be recycled using the same fusion mechanism. However, when the detector D$_1$ detects photon, the state of the system is changed as

$$|\phi_2\rangle = \left(|a\rangle|c\rangle|\uparrow\rangle_1|\uparrow\rangle_2 + |a\rangle|d\rangle|\uparrow\rangle_1|\downarrow\rangle_2 + |b\rangle|c\rangle|\downarrow\rangle_1|\uparrow\rangle_2\right) \otimes |R_2\rangle. \quad (8)$$

$|\phi_2\rangle$ is used to continue the fusion process. Now, let the photon 2 pass through c-PBS$_1$ and interact with the spin 1. After passing though c-PBS$_1$ again, we obtain

$$|\phi_3\rangle = |R_2\rangle|a\rangle|c\rangle|\uparrow\rangle_1|\uparrow\rangle_2 + |R_2\rangle|a\rangle|d\rangle|\uparrow\rangle_1|\downarrow\rangle_2 + |L_2\rangle|b\rangle|c\rangle|\downarrow\rangle_1|\uparrow\rangle_2. \quad (9)$$

Then, the photon 2 exits from the optical switch and goes towards c-PBS$_6$. The component $|R_2\rangle$ transmits c-PBS$_6$ and does not interact with the spin 2 and spin 1. However, the component $|L_2\rangle$ passes through HWP$_1$ which realizes $|R\rangle \rightarrow (|R\rangle + |L\rangle)/\sqrt{2}$ and $|L\rangle \rightarrow (|R\rangle - |L\rangle)/\sqrt{2}$, and then enters cavity 2 via c-PBS$_5$ to interact with the spin 2. It is worth noting that before and after the photon 2 interacts with the electron spin 2, a Hadamard operation (H$_e$) on the electron spin 2 is performed by a $\pi/2$ microwave pulse or an optical pulse[23,40], i.e. $\left\{|\uparrow\rangle_s \rightarrow \left(|\uparrow\rangle_s + |\downarrow\rangle_s\right)/\sqrt{2}, |\downarrow\rangle_s \rightarrow \left(|\uparrow\rangle_s - |\downarrow\rangle_s\right)/\sqrt{2}\right\}$. With operations $\left(c-\mathrm{PBS}_6 \rightarrow \mathrm{HWP}_1 \rightarrow c-\mathrm{PBS}_5 \rightarrow \mathrm{H}_e \rightarrow \begin{Bmatrix}\mathrm{L}_2 \rightarrow \mathrm{PS} \rightarrow \mathrm{spin1}\\ \mathrm{R}_2 \rightarrow \mathrm{spin1} \rightarrow \mathrm{PS}\end{Bmatrix} \rightarrow \mathrm{H}_e\right)$, the photon-electron state can evolve as

$$|\phi_4\rangle = |R_2\rangle|a\rangle|c\rangle|\uparrow\rangle_1|\uparrow\rangle_2 + |R_2\rangle|a\rangle|d\rangle|\uparrow\rangle_1|\downarrow\rangle_2 + \frac{|b\rangle|c\rangle}{\sqrt{2}}|\downarrow\rangle_1\left(|R_2\rangle|\downarrow\rangle_2 - |L_2\rangle|\downarrow\rangle_2\right). \quad (10)$$

Whereafter, the photon passes c-PBS$_7$ and PS, successively. Before and after interacting with the spin 1, we performs a Hadamard gate on electron spin 1. Then the photon 2 passes through the HWP$_2$. With these operations (c-PBS$_7 \rightarrow$ H$_e \rightarrow$ spin $1 \rightarrow$ H$_e \rightarrow$ HWP$_2$), we obtain

$$|\phi_5\rangle = |R_2\rangle|a\rangle|c\rangle|\uparrow\rangle_1|\uparrow\rangle_2 + |R_2\rangle|a\rangle|d\rangle|\uparrow\rangle_1|\downarrow\rangle_2 + |L_2\rangle|b\rangle|c\rangle|\uparrow\rangle_1|\downarrow\rangle_2. \quad (11)$$

Due to the DL, the photon components exit from c-PBS$_7$ and c-PBS$_6$ and arrive the OWM at the same time. QWP is a quarter-wave plate which implements transformations $|R\rangle \rightarrow |V\rangle$ and $|L\rangle \rightarrow |H\rangle$. P$_{45}$ is a 45° polarizer[41] projecting the polarization to $(|H\rangle + |V\rangle)/\sqrt{2}$. The photon passing through the OWM, QWP and P$_{45}$ in turn. As long as the photon detector D$_3$ clicks, the resulting state of the total spin-photon system becomes as:

$$|\phi_6\rangle = |\uparrow\rangle_1\left(|a\rangle|c\rangle|\uparrow\rangle_2 + |a\rangle|d\rangle|\downarrow\rangle_2 + |b\rangle|c\rangle|\downarrow\rangle_2\right). \quad (12)$$

It is clearly that electron spin 1 is disentangled with other electron spins. Therefore the state of the remaining electron spins is given by

$$\begin{aligned}|\phi_7\rangle &= |a\rangle|c\rangle|\uparrow\rangle_2 + |a\rangle|d\rangle|\downarrow\rangle_2 + |b\rangle|c\rangle|\downarrow\rangle_2\\ &= \frac{1}{\sqrt{nm}}\Big[\left|(n-1)_\downarrow\right\rangle_a\left|(m-1)_\downarrow\right\rangle_b|1_\uparrow\rangle_2 + \sqrt{m-1}\left|(n-1)_\downarrow\right\rangle_a|W_{m-1}\rangle_b\left|1_\downarrow\right\rangle_2\\ &\quad + \sqrt{n-1}\,|W_{n-1}\rangle_a\left|(m-1)_\downarrow\right\rangle_b|1_\uparrow\rangle_2\Big]\\ &= \frac{\sqrt{n+m-1}}{\sqrt{nm}}|W_{n+m-1}\rangle. \end{aligned} \quad (13)$$

Obviously, $|\phi_6\rangle$ is a W state with $n+m-1$ electrons (i.e., $|W_{n+m-1}\rangle$), and the probability obtaining the W state is $(n+m-1)/nm$. Here we have used $\sqrt{k}\,|W_k\rangle = \sqrt{i}\,|W_i\rangle\left|(k-i)_\downarrow\right\rangle + \sqrt{k-i}\left|i_\downarrow\right\rangle|W_{k-i}\rangle$.

Photonic *W*-state Fusion based on QD-microcavity coupled system. In this section, we will introduce the fusion protocol of the photonic W-state in detail. The schematic is depicted in Fig. 3. We use the similar notation $|W_n\rangle_A$ and $|W_m\rangle_B$ as electronic W states in the above section,

$$\begin{aligned}|W_n\rangle_A &= \frac{1}{\sqrt{n}}\Big[\left|(n-1)_L\right\rangle_a|1_R\rangle_1 + \sqrt{n-1}\,|W_{n-1}\rangle_a|1_L\rangle_1\Big]\\ &= |a\rangle|R\rangle_1 + |b\rangle|L\rangle_1, \end{aligned} \quad (14)$$

$$\begin{aligned}|W_m\rangle_B &= \frac{1}{\sqrt{m}}\Big[\left|(m-1)_L\right\rangle_b|1_R\rangle_2 + \sqrt{m-1}\,|W_{m-1}\rangle_b|1_L\rangle_2\Big].\\ &= |c\rangle|R\rangle_2 + |d\rangle|L\rangle_2. \end{aligned} \quad (15)$$

Distinctly, a tripartite W state is written as $|W_3\rangle_A = \left(|LLR\rangle_A + |LRL\rangle_A + |RLL\rangle_A\right)/\sqrt{3} = \left(|2_L\rangle_a|1_R\rangle_1 + \sqrt{2}\,|W_2\rangle_a|1_L\rangle_1\right)/\sqrt{3}$ with $|W_2\rangle$ corresponding to the EPR pair $|W_2\rangle = (|LR\rangle + |RL\rangle)/\sqrt{2}$. For simplicity, here we have substituted $|a\rangle$ for $\left|(n-1)_L\right\rangle_a/\sqrt{n}$, $|b\rangle$ for $\sqrt{n-1}/\sqrt{n}\,|W_{n-1}\rangle_a$, $|c\rangle$ for $\left|(m-1)_L\right\rangle_b/\sqrt{m}$, and $|d\rangle$ for

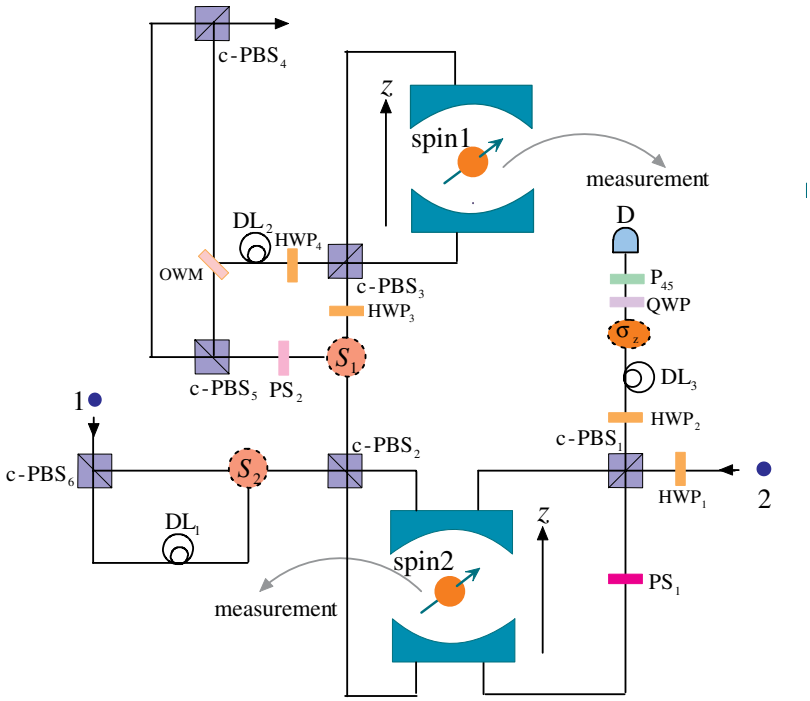

Figure 3. Schematic of photonic *W*-state fusion. All the optical elements are the same as Fig. 2.

$\sqrt{(m-1)}\,/\sqrt{m}\,|W_{m-1}\rangle_b$. Our scheme is based on the QD double-side optical microcavity, the electron spin 1 (electron spin 2) is initially in the state $|\uparrow\rangle_1\left(|\uparrow\rangle_2\right)$. Therefore the initial state can be written as:

$$\begin{aligned}|\Psi_0\rangle &= |W_n\rangle_A \otimes |W_m\rangle_B \otimes |\uparrow\rangle_1 \otimes |\uparrow\rangle_2 \\ &= \left(|a\rangle|R\rangle_1 + |b\rangle|L\rangle_1\right) \otimes \left(|c\rangle|R\rangle_2 + |d\rangle|L\rangle_2\right)|\uparrow\rangle_1|\uparrow\rangle_2. \end{aligned} \tag{16}$$

In our fusion scheme, only the photons in mode 1 and 2 are sent to the fusion device and the remaining photons in modes a (b) are kept constant at Alice's (Bob's) side. In other words, only $|1_R\rangle_1|1_R\rangle_2$, $|1_L\rangle_1|1_R\rangle_2$, $|1_R\rangle_1|1_L\rangle_2$, and $|1_L\rangle_1|1_L\rangle_2$ are sent to the fusion mechanism with the probabilities $P_{RR}=1/(nm)$, $P_{LR}=(n-1)/(nm)$, $P_{RL}=(m-1)/(nm)$, and $P_{LL}=(n-1)(m-1)/(nm)$, respectively.

Before and after the photon 2 passes through the second optical microcavity, Hadamard operations H_p and H_e are performed on photon 2 and electron 2, respectively. PS_1 realizes the transformations $\{|R\rangle \rightarrow -|R\rangle,\ \ |L\rangle \rightarrow -|L\rangle\}$. After these operations $\left(\mathrm{HWP_1} \rightarrow \mathrm{H}_e \rightarrow \begin{Bmatrix}\mathrm{L_2} \rightarrow \mathrm{PS_1} \rightarrow \mathrm{spin2} \\ \mathrm{R_2} \rightarrow \mathrm{spin2} \rightarrow \mathrm{PS_1}\end{Bmatrix} \rightarrow \mathrm{H}_e \rightarrow \mathrm{HWP_2}\right)$, the state of the photon-electron system is given by

$$|\Psi_1\rangle = \left(|a\rangle|R\rangle_1|\uparrow\rangle_1 + |b\rangle|L\rangle_1|\uparrow\rangle_1\right)\left(|c\rangle|R\rangle_2|\uparrow\rangle_2 + |d\rangle|L\rangle_2|\downarrow\rangle_2\right). \tag{17}$$

Now, the photon 1 passes through the c-PBS_6, the component $|R_1\rangle$ does not interact with the spin 2 and spin 1 while the component $|L_1\rangle$ passes through the optical switch S_2 and the c-PBS_2. Then it enters cavity 2 and interacts with the spin 2. These operations (c-$PBS_6 \rightarrow S_2 \rightarrow$ c-$PBS_2 \rightarrow$ spin 2 $\rightarrow$ c-PBS_2) make $|\Psi_1\rangle$ become

$$\begin{aligned}|\Psi_2\rangle &= |a\rangle|R\rangle_1|\uparrow\rangle_1\left(|c\rangle|R\rangle_2|\uparrow\rangle_2 + |d\rangle|L\rangle_2|\downarrow\rangle_2\right) \\ &\quad - |b\rangle|c\rangle|L\rangle_1|R\rangle_2|\uparrow\rangle_1|\uparrow\rangle_2 + |b\rangle|d\rangle|R\rangle_1|L\rangle_2|\uparrow\rangle_1|\downarrow\rangle_2. \end{aligned} \tag{18}$$

Next, the photon 1 goes through the optical switch S_1, HWP_3, c-PBS_3, one by one. Before and after the photon 1 interacts with the electron spin 1, a Hadamard operation H_e is performed on the electron spin 1 by using a $\pi/2$ microwave pulse or an optical pulse. Then photon 1 passes HWP_4. After these operations ($S_1 \rightarrow HWP_3 \rightarrow H_e \rightarrow$ c-$PBS_3 \rightarrow$ spin 1 $\rightarrow H_e \rightarrow$ c-$PBS_3 \rightarrow HWP_4$), the state becomes

$$|\Psi_2\rangle = |\uparrow\rangle_1\big(|a\rangle|c\rangle|R\rangle_1|R\rangle_2|\uparrow\rangle_2 + |a\rangle|d\rangle|R\rangle_1|L\rangle_2|\downarrow\rangle_2 + |b\rangle|c\rangle|L\rangle_1|R\rangle_2|\downarrow\rangle_2\big) - |b\rangle|d\rangle|R\rangle_1|L\rangle_2|\downarrow\rangle_1|\downarrow\rangle_2. \quad (19)$$

Here, a measurement is performed on the electron spin 1 which has two possible results as below

$$\begin{aligned} &|\downarrow\rangle_1: |\psi_1\rangle = -|b\rangle|d\rangle|R\rangle_1|L\rangle_2|\downarrow\rangle_2, \\ &|\uparrow\rangle_1: |\psi_2\rangle = |a\rangle|c\rangle|R\rangle_1|R\rangle_2|\uparrow\rangle_2 + |a\rangle|d\rangle|R\rangle_1|L\rangle_2|\downarrow\rangle_2 + |b\rangle|c\rangle|L\rangle_1|R\rangle_2|\uparrow\rangle_2. \end{aligned} \quad (20)$$

For the result $|\downarrow\rangle_1$, we will get two separate W states with a smaller number of qubits, $|W_{n-1}\rangle$ and $|W_{m-1}\rangle$, which can be recycled by the same fusion mechanism. For the other situation we acquire $|\psi_2\rangle$, it will be used to continue the fusion process. At this time, the component $|R_1\rangle$ in the DL_1 passes through the optical switch S_2, c-PBS$_2$ and enters the spin 2. When the photon leaves away from the cavity 2, it passes through the switch S_1 and interacts with PS$_2$ which implements the transformations $\{|R\rangle \rightarrow -|R\rangle, |L\rangle \rightarrow |L\rangle\}$. After these operations (c-PBS$_2$ → spin 2 → c-PBS$_2$ → S_1 → PS$_2$ → c-PBS$_5$ → OWM), the photon-electron state evolves as

$$|\Psi_3\rangle = |a\rangle|c\rangle|R\rangle_1|R\rangle_2|\uparrow\rangle_2 + |a\rangle|d\rangle|L\rangle_1|L\rangle_2|\downarrow\rangle_2 + |b\rangle|c\rangle|L\rangle_1|R\rangle_2|\uparrow\rangle_2. \quad (21)$$

Here, the DL$_2$ makes the components of photon 1 which exit from the HWP$_4$ and PBS$_5$, respectively, to arrive the OWM at the same time. Now, all the components of the photon 1 are combined at c-PBS$_4$.

Then we perform a Hadamard gate on electron spin 2 and measure it in basis $\{|\uparrow\rangle, |\downarrow\rangle\}$. If the measurement result is $|\uparrow\rangle$, the state of the remaining system is

$$|\Psi_4\rangle = |a\rangle|c\rangle|R\rangle_1|R\rangle_2 + |a\rangle|d\rangle|L\rangle_1|L\rangle_2 + |b\rangle|c\rangle|L\rangle_1|R\rangle_2. \quad (22)$$

Now, the photon 2 derectly passes through QWP and P$_{45}$ in turn. When the photon detector D clicks, the resulting state of the remaining photons becomes as below:

$$\begin{aligned} |\Psi_5\rangle &= |a\rangle|c\rangle|R\rangle_1 + |a\rangle|d\rangle|L\rangle_1 + |b\rangle|c\rangle|L\rangle_1 \\ &= \frac{1}{\sqrt{nm}}\Big[\Big|(n-1)_L\Big\rangle_a\Big|(m-1)_L\Big\rangle_b|1_R\rangle_1 + \sqrt{m-1}\Big|(n-1)_L\Big\rangle_a|W_{m-1}\rangle_b|1_L\rangle_1 \\ &\quad + \sqrt{n-1}\,|W_{n-1}\rangle_a\Big|(m-1)_L\Big\rangle_b|1_L\rangle_1\Big] \\ &= \frac{\sqrt{n+m-1}}{\sqrt{nm}}|W_{n+m-1}\rangle, \end{aligned} \quad (23)$$

which is a W state with $n+m-1$ photons, i.e. $|W_{n+m-1}\rangle$, where we have used $\sqrt{k}\,|W_k\rangle = \sqrt{i}\,|W_i\rangle|(k-i)_L\rangle + \sqrt{k-i}\,|i_L\rangle|W_{k-i}\rangle$. If the electron 2 is in $|\downarrow\rangle$, we have

$$|\Psi_6\rangle = |a\rangle|c\rangle|R\rangle_1|R\rangle_2 - |a\rangle|d\rangle|L\rangle_1|L\rangle_2 + |b\rangle|c\rangle|L\rangle_1|R\rangle_2, \quad (24)$$

The σ_z operation on the photon 2 is needed before it passes through QWP, and the state of photons will become the same as Eq. (22). With the same operation above, we can obtain a $(n+m-1)$-qubit W state in Eq. (23) with the probability $(n+m-1)/nm$. So far, we have completed the W-state fusion schemes for electronic and photonic W state, respectively, based on the quantum-dot-microcavity coupled system.

Discussion

In this section, we will briefly analyze and discuss the feasibility and the success probability of the proposed schemes. When the side leakage and cavity loss are taken into account, the reflection and transmission coefficients of the coupled and the uncoupled cavities are generally different in a realistic X^--cavity system. The reflection and transmission coefficients of a double-sided optical microcavity for weak excitation limit can be described by[26,27]

$$\begin{aligned} r(\omega) &= \frac{\left[i(\omega_{X^-}-\omega)+\frac{\gamma}{2}\right]\left[i(\omega_c-\omega)+\frac{\kappa_s}{2}\right]+g^2}{\left[i(\omega_{X^-}-\omega)+\frac{\gamma}{2}\right]\left[i(\omega_c-\omega)+\kappa+\frac{\kappa_s}{2}\right]+g^2}, \\ t(\omega) &= \frac{-\kappa\left[i(\omega_{X^-}-\omega)+\frac{\gamma}{2}\right]}{\left[i(\omega_{X^-}-\omega)+\frac{\gamma}{2}\right]\left[i(\omega_c-\omega)+\kappa+\frac{\kappa_s}{2}\right]+g^2}, \end{aligned} \quad (25)$$

here g is the coupling strength, κ, κ_s, and γ are the cavity field decay rate, leaky rate, and X^- dipole decay rate, respectively. ω, ω_c, and ω_{X^-} are the frequencies of the input photon, cavity mode, and the

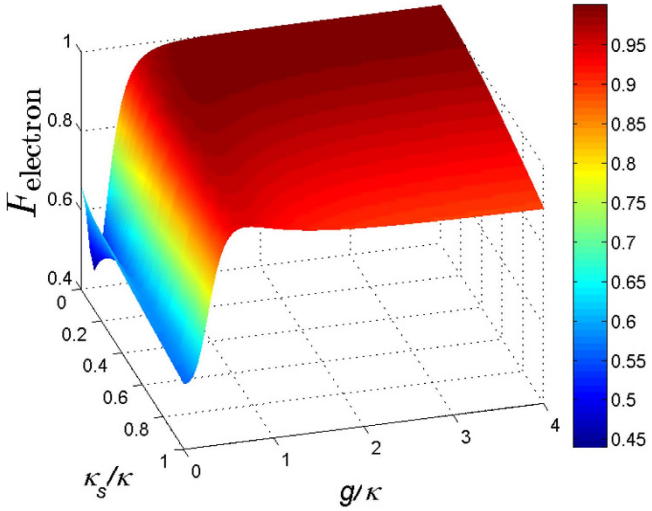

Figure 4. The fidelity of the electronic *W*-state fusion scheme versus the normalized coupling strengths g/κ and side leakage rate κ_s/κ, where we have set $\gamma = 0.1\kappa$.

spin-dependent optical transition, respectively. By setting $\omega_c = \omega_{X^-} = \omega$, the reflection and transmission coefficients of the coupled cavity is given by

$$r(\omega) = \frac{\gamma\kappa_s + 4g^2}{\gamma(2\kappa + \kappa_s) + 4g^2}, \qquad t(\omega) = -\frac{2\gamma\kappa}{\gamma(2\kappa + \kappa_s) + 4g^2}, \tag{26}$$

and uncoupled cavity ($g = 0$) is

$$r_0(\omega) = \frac{\kappa_s}{2\kappa + \kappa_s}, \qquad t_0(\omega) = -\frac{2\kappa}{2\kappa + \kappa_s}. \tag{27}$$

Therefore, in a realistic spin-QD-double-side-cavity unit, the rules of the optical transitions can be described as

$$\begin{aligned}
|R^{\downarrow}, \uparrow\rangle &\rightarrow -|t_0(\omega)||R^{\downarrow}, \uparrow\rangle - |r_0(\omega)||L^{\uparrow}, \uparrow\rangle,\\
|L^{\uparrow}, \uparrow\rangle &\rightarrow -|t_0(\omega)||L^{\uparrow}, \uparrow\rangle - |r_0(\omega)||R^{\downarrow}, \uparrow\rangle,\\
|R^{\downarrow}, \downarrow\rangle &\rightarrow |r(\omega)||L^{\uparrow}, \downarrow\rangle + |t(\omega)||R^{\downarrow}, \downarrow\rangle,\\
|L^{\uparrow}, \downarrow\rangle &\rightarrow |r(\omega)||R^{\downarrow}, \downarrow\rangle + |t(\omega)||L^{\uparrow}, \downarrow\rangle.
\end{aligned} \tag{28}$$

The fidelity of the fusion scheme is $F = \left|\langle\Psi_s|\Psi_t\rangle\right|^2$, in which $|\Psi_s\rangle$ and $|\Psi_t\rangle$ represent the final states of the present fusion scheme in the realistic condition and the ideal condition, respectively. Figures 4 and 5 are the fidelities of electronic and photonic *W*-state fusion schemes (F_{electron} and F_{photonic}), respectively, which show our schemes can be achieved with high fidelities. Nevertheless, the cavity side leakage and cavity field decay have obvious impact on the fusion-scheme fidelities. Fortunately, the strong coupling of the QD-microcavity system has been observed in[42–45]. And the improvement of fabrication techniques can suppress the side leakage which reported $g/(\kappa + \kappa_s) \simeq 0.5$ and $g/(\kappa + \kappa_s) \simeq 2.4$. In our scheme, if setting $\kappa_s = 0.5\kappa$, $g = 2.5\kappa$, (i.e. $g/(\kappa + \kappa_s) \simeq 1.7$ which is the strong coupling regime) we can obtain $F_{\text{electron}} = 99.99\%$, $F^a_{\text{photon}} = 99.99\%$, and $F^b_{\text{photon}} = 99.99\%$; even when setting $\kappa_s = 1.0\kappa$, $g = 0.4\kappa$, (i.e. $g/(\kappa + \kappa_s) = 0.2$ which is the weak coupling regime) we also can obtain $F_{\text{electron}} = 87.55\%$, $F^a_{\text{photon}} = 72.68\%$, and $F^b_{\text{photon}} = 77.26\%$. Therefore, our scheme can work well in both the weak coupling and the strong coupling regimes.

In addition, the electron spin decoherence and the exciton dephasing could also effect the fidelity. Exciton dephasing reduces the fidelity by the amount of $1 - e^{-\frac{\tau}{T_e}}$, where τ is the photon life time in the cavity and T_e is the exciton coherence time[26,27]. The optical dephasing reduces the fidelity only a few percent that is because in a self-assembled In(Ga)As-based QD the time scale of the excitons can reach hundreds of picoseconds[45–47]. The effect of the spin dephasing is mainly due to the hole-spin dephasing, while the hole spin coherence time is at least three orders of magnitude longer than the cavity photon lifetime[48], so the spin dephasing can be safely neglected.

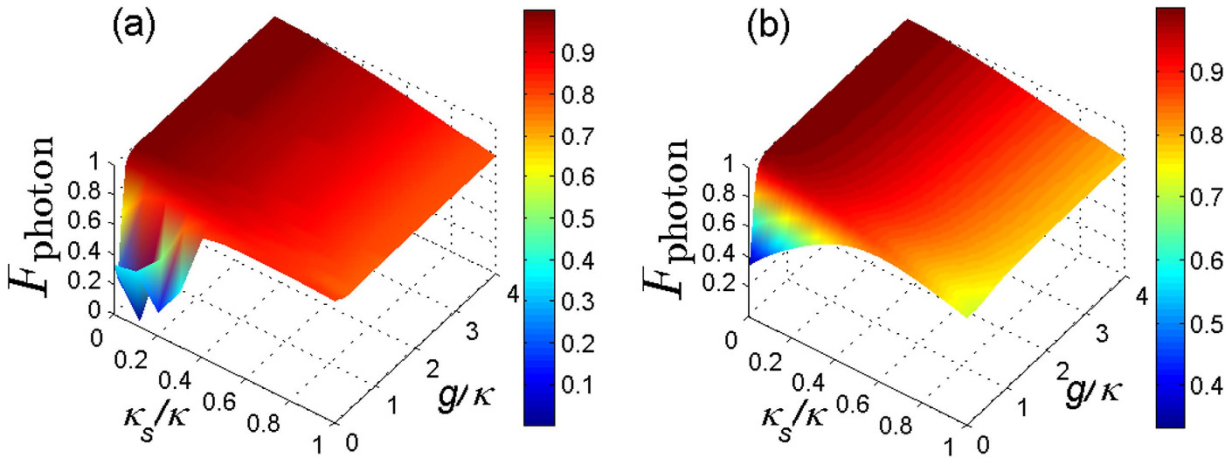

Figure 5. The fidelity of the photonic *W*-state fusion scheme versus the normalized coupling strengths g/κ and side leakage rate κ_s/κ. (**a**) The fidelity corresponding to that the measurement result of the electron spin is $|\uparrow\rangle_s$. (**b**) The fidelity corresponding to that the measurement result of the electron spin is $|\downarrow\rangle_s$. Here we have set $\gamma = 0.1\kappa$.

Obviously, in the whole fusion process, the fused large *W* state is from the items of the initial state with the electron (photon) 1 and 2 in the states $|1_\uparrow\rangle_1 |1_\downarrow\rangle_2$, $|1_\downarrow\rangle_1 |1_\uparrow\rangle_2$, and $|1_\uparrow\rangle_1 |1_\downarrow\rangle_2$ ($|1_R\rangle_1|1_R\rangle_2$, $|1_L\rangle_1|1_R\rangle_2$, and $|1_R\rangle_1|1_L\rangle_2$). While the item with the electron (photon) 1 and 2 in $|1_\downarrow\rangle_1|1_\downarrow\rangle_2$ ($|1_L\rangle_1|1_L\rangle_2$) would become two smaller *W* states after measuring the photon 1 (electron 1), which can be recycled using the same fusion mechanism. Therefore the success probability P_s and the recyclable probability P_r are written as

$$P_s = \frac{(n-1)}{(nm)} + \frac{(m-1)}{(nm)} + \frac{1}{(nm)} = \frac{n+m-1}{nm},$$
$$P_r = \frac{(n-1)(m-1)}{nm}. \tag{29}$$

Therefore, the fusion schemes for electronic and photonic *W* state could be effectively implemented with the success probability $(n+m-1)/nm$.

Methods

Input-output relation of QD double-sided cavity system. The reflection and transmission coefficients of the QD-cavity system can be calculated from the Heisenberg equations of motion for the cavity field operator $\hat{a}$ and X^- dipole operator σ_- in the interaction picture[49]

$$\begin{aligned}
\frac{d\hat{a}}{dt} &= -\left[i(\omega_c - \omega) + \kappa + \frac{\kappa_s}{2}\right]\hat{a} - g\hat{\sigma}_- - \sqrt{\kappa}\,\hat{a}_{in} - \sqrt{\kappa}\,\hat{a}'_{in},\\
\frac{d\hat{\sigma}_-}{dt} &= -\left[i(\omega_{X^-} - \omega) + \frac{\gamma}{2}\right]\hat{\sigma}_- - g\hat{\sigma}_z\hat{a},\\
\hat{a}_r &= \hat{a}_{in} + \sqrt{\kappa}\,\hat{a},\\
\hat{a}_t &= \hat{a}'_{in} + \sqrt{\kappa}\,\hat{a}.
\end{aligned} \tag{30}$$

where $\hat{a}_{in}$, $\hat{a}'_{in}$ and $\hat{a}_r$, $\hat{a}_t$ are the two input and the two output fields operators of the double-side cavity, respectively. And other parameters are the same as Eq. (25). The reflection and transmission coefficients in Eq. (25) can be obtained in the approximation of weak excitation where the charged QD is predominantly in the ground state with $\langle\hat{\sigma}_z\rangle = -1$.

Manipulation and measurement of the electron spin in QD. The Hadamard transformation and projective measurement on the electron spin are needed in the present schemes. The Hadamard transformation $\{|\uparrow\rangle \to (|\uparrow\rangle + |\downarrow\rangle)/\sqrt{2}, |\downarrow\rangle \to (|\uparrow\rangle - |\downarrow\rangle)/\sqrt{2}\}$ can be implemented by using a $\pi/2$ microwave or optical pulse[23,50,51]. The projection measurement of the electron spin can be achieved with the help of an auxiliary circularly polarized photon. If a right-circularly polarized photon $|R\rangle$ is

initially sent into the cavity along the z axis, after interacting with QD-cavity system, the joint state of the photon and electron becomes

$$|R^{\uparrow}, \uparrow\rangle \rightarrow |L^{\downarrow}, \uparrow\rangle, \quad |R^{\uparrow}, \downarrow\rangle \rightarrow -|R^{\uparrow}, \downarrow\rangle. \tag{31}$$

Obviously, the projection measurement of the electron spin can be completed by detecting the reflection and transmission of the photon. The electron spin is projected into the state $|\uparrow\rangle$ for photon's reflection; the electron spin is projected into the state $|\downarrow\rangle$ for photon's transmission.

References

1. Bennett, C. H. *et al.* Teleporting an unknown quantum state via dual classical and Einstein-Podolsky-Rosen channels. *Phys. Rev. Lett.* **70,** 1895–1899 (1993).
2. Ekert, A. K. Quantum cryptography based on Bell's theorem. *Phys. Rev. Lett.* **67,** 661–663 (1991).
3. Nielsen, M. A. & Chuang, I. L. *Quantum computation and quantum information*. (Cambridge university press, Cambridge, U.K., 2000).
4. Gräfe, M. *et al.* On-chip generation of high-order single-photon *W*-states. *Nat. Photonics* **8,** 791–795 (2014).
5. Ng, H. T. & Kim, K. Quantum estimation of magnetic-field gradient using *W*-state. *Opt. Commun.* **331,** 353–358 (2014).
6. Ozaydin, F. Phase damping destroys quantum Fisher information of *W* states. *Phys. Lett. A* **378,** 3161–3164 (2014).
7. Yu, N., Guo, C. & Duan, R. Obtaining a *W* state from a Greenberger-Horne-Zeilinger state via stochastic local operations and classical communication with a rate approaching unity. *Phys. Rev. Lett.* **112,** 160401 (2014).
8. Murao, M., Jonathan, D., Plenio, M. B. & Vedral, V. Quantum telecloning and multiparticle entanglement. *Phys. Rev. A* **59,** 156–161 (1999).
9. Joo, J., Lee, J., Jang, J. & Park, Y. J. Quantum secure communication with *W* States. arXiv:quant-ph/0204003v2.
10. Browne, D. E. & Rudolph, T. Resource-efficient linear optical quantum computation. *Phys. Rev. Lett.* **95,** 010501 (2005).
11. Zeilinger, A., Horne, M. A., Weinfurter, H. & Żukowski, M. Three-particle entanglements from two entangled pairs. *Phys. Rev. Lett.* **78,** 3031–3034 (1997).
12. Tashima, T. *et al.* Demonstration of local expansion toward large-scale entangled webs. *Phys. Rev. Lett.* **105,** 210503 (2010).
13. Tashima, T., Özdemir, Ş. K., Yamamoto, T., Koashi, M. & Imoto, N. Elementary optical gate for expanding an entanglement web. *Phys. Rev. A* **77,** 030302 (2008).
14. Tashima, T., Özdemir, Ş. K., Yamamoto, T., Koashi, M. & Imoto, N. Local expansion of photonic *W* state using a polarization-dependent beamsplitter. *New J. Phys.* **11,** 023024 (2009).
15. Tashima, T. *et al.* Local transformation of two Einstein-Podolsky-Rosen photon pairs into a three-photon *W* State. *Phys. Rev. Lett.* **102,** 130502 (2009).
16. Özdemir, Ş. K. *et al.* An optical fusion gate for *W*-states. *New J. Phys.* **13,** 103003 (2011).
17. Bugu, S., Yesilyurt, C. & Ozaydin, F. Enhancing the *W*-state quantum-network-fusion process with a single Fredkin gate. *Phys. Rev. A* **87,** 032331 (2013).
18. Yesilyurt, C., Bugu, S. & Ozaydin, F. An optical gate for simultaneous fusion of four photonic *W* or Bell states. *Quant. Inf. Process.* **12,** 2965–2975 (2013).
19. Ozaydin, F. *et al.* Fusing multiple *W* states simultaneously with a Fredkin gate. *Phys. Rev. A* **89,** 042311 (2014).
20. Han, X., Hu, S., Guo, Q., Wang, H. F. & Zhang, S. Effective scheme for *W*-state fusion with weak cross-Kerr nonlinearities. *Quant. Inf. Process.* doi: 10.1007/s11128-015-0960-x.
21. Emary, C., Xu, X. D., Steel, D. G., Saikin, S. & Sham, L. J. Fast initialization of the spin state of an electron in a quantum dot in the Voigt configuration. *Phys. Rev. Lett.* **98,** 047401 (2007).
22. Kim, D. *et al.* Optical spin initialization and nondestructive measurement in a quantum dot molecule. *Phys. Rev. Lett.* **101,** 236804 (2008).
23. Press, D., Ladd, T. D., Zhang, B. & Yamamoto, Y. Complete quantum control of a single quantum dot spin using ultrafast optical pulses. *Nature (London)* **456,** 218–221 (2008).
24. Kim, E. D. *et al.* Fast spin rotations by optically controlled geometric phases in a charge-tunable InAs quantum dot. *Phys. Rev. Lett.* **104,** 167401 (2010).
25. Bonato, C. *et al.* CNOT and Bell-state analysis in the weak-coupling cavity QED regime. *Phys. Rev. Lett.* **104,** 160503 (2010).
26. Hu, C. Y., Munro, W. J., O'Brien, J. L. & Rarity, J. G. Proposed entanglement beam splitter using a quantum-dot spin in a double-sided optical microcavity. *Phys. Rev. B* **80,** 205326 (2009).
27. Hu, C. Y. & Rarity, J. G. Loss-resistant state teleportation and entanglement swapping using a quantum-dot spin in an optical microcavity. *Phys. Rev. B* **83,** 115303 (2011).
28. Ren, B. C., Wei, H. R., Hua, M., Li, T. & Deng, F. G. Complete hyperentangled-Bell-state analysis for photon systems assisted by quantum-dot spins in optical microcavities. *Opt. Express* **20,** 24664 (2012).
29. Wang, H. F., Zhu, A. D., Zhang, S. & Yeon, K. H. Physical optimization of quantum error correction circuits with spatially separated quantum dot spins. *Opt. Express* **21,** 12484 (2013).
30. Guo, Q., Cheng, L. Y., Chen, L., Wang, H. F. & Zhang, S. Counterfactual entanglement distribution without transmitting any particles. *Opt. Express* **22,** 12484 (2014).
31. Wang, T. J., Song, S. Y. & Long, G. L. Quantum repeater based on spatial entanglement of photons and quantum-dot spins in optical microcavities. *Phys. Rev. A* **85,** 062311 (2012).
32. Wang, H. F., Zhu, A. D., Zhang, S. & Yeon, K. H. Optically controlled phase gate and teleportation of a controlled-not gate for spin qubits in a quantum-dotšCmicrocavity coupled system. *Phys. Rev. A* **87,** 062337 (2013).
33. Wei, H. R. & Deng, F. G. Universal quantum gates for hybrid systems assisted by quantum dots inside double-sided optical microcavities. *Phys. Rev. A* **87,** 022305 (2013).
34. Guo, Q., Cheng, L. Y., Chen, L., Wang, H. F. & Zhang, S. Counterfactual distributed controlled-phase gate for quantum-dot spin qubits in double-sided optical microcavities. *Phys. Rev. A* **90,** 8970–8984 (2014).
35. Wei, H. R. & Deng, F. G. Scalable photonic quantum computing assisted by quantum-dot spin in double-sided optical microcavity. *Opt. Express* **21,** 17671 (2013).
36. Ren, B. C. & Deng, F. G. Hyper-parallel photonic quantum computation with coupled quantum dots. *Sci. Rep.* **4,** 4623 (2014).
37. Wei, H. R. & Deng, F. G. Scalable quantum computing based on stationary spin qubits in coupled quantum dots inside double-sided optical microcavities. *Sci. Rep.* **4,** 7551 (2014).
38. Dong, L., Xiu, X. M., Gao, Y. J. & Yi, X. X. A nearly deterministic scheme for generating χ-type entangled states with weak cross-Kerr nonlinearities. *Quant. Inf. Process.* **12,** 1787–1795 (2013).

39. Zhang, W., Rui, P., Zhang, Z. Y. & Yang, Q. Probabilistically cloning two single-photon states using weak cross-Kerr nonlinearities. *New J. Phys.* **16,** 083019 (2014).
40. Hu, C. Y., Young, A., O'Brien, J. L., Munro, W. J. & Rarity, J. G. Giant optical Faraday rotation induced by a single-electron spin in a quantum dot: applications to entangling remote spins via a single photon. *Phys. Rev. B* **78,** 085307 (2008).
41. Chen, Q. & Feng, M. Quantum-information processing in decoherence-free subspace with low-*Q* cavities. *Phys. Rev. A* **82,** 052329 (2010).
42. Reithmaier, J. P. *et al.* Strong coupling in a single quantum dot-semiconductor microcavity system. *Nature (London)* **432,** 197–200 (2004).
43. Yoshie, T. *et al.* Vacuum Rabi splitting with a single quantum dot in a photonic crystal nanocavity. *Nature (London)* **432,** 200–203 (2004).
44. Peter, E. *et al.* Exciton-photon strong-coupling regime for a single quantum dot embedded in a microcavity. *Phys. Rev. Lett.* **95,** 067401 (2005).
45. Reitzenstein, S. *et al.* AlAs/GaAs micropillar cavities with quality factors exceeding 150.000. *Appl. Phys. Lett.* **90,** 251109 (2007).
46. Borri, P. *et al.* Ultralong dephasing time in InGaAs quantum dots. *Phys. Rev. Lett.* **87,** 157401 (2001).
47. Langbein, W. *et al.* Radiatively limited dephasing in InAs quantum dots. *Phys. Rev. B* **70,** 033301 (2004).
48. Brunner, D. *et al.* A coherent single-hole spin in a semiconductor. *Science* **325,** 70–72 (2009).
49. Walls, D. F. & Milburn, G. J. *Quantum Optics* (Springer-Verlag, Berlin, 1994).
50. Berezovsky, J., Mikkelsen, M. H., Stoltz, N. G., Coldren, L. A. & Awschalom, D. D. Picosecond coherent optical manipulation of a single electron spin in a quantum dot. *Science* **320,** 349–352 (2008).
51. Greilich, A. *et al.* Ultrafast optical rotations of electron spins in quantum dots. *Nature Phys.* **5,** 262 (2009).

Acknowledgements

This work is supported by the National Natural Science Foundation of China under Grant Nos. 61465013, 11465020, 11165015, and 11264042; the Program for Chun Miao Excellent Talents of Jilin Provincial Department of Education under Grant No. 201316; and the Talent Program of Yanbian University of China under Grant No. 950010001.

Author Contributions

X.H. designed the scheme under the guidance of H.F., A.D. and S.Z. X.H., S.H. and Q.G. carried out the theoretical analysis. All authors contributed to the interpretation of the work and the writing of the manuscript. All authors reviewed the manuscript.

Additional Information

Competing financial interests: The authors declare no competing financial interests.

How to cite this article: Han, X. *et al.* Effective *W*-state fusion strategies for electronic and photonic qubits via the quantum-dot-microcavity coupled system. *Sci. Rep.* **5**, 12790; doi: 10.1038/srep12790 (2015).